PHYSICAL REVIEW LETTERS

Dissociative Electron Attachment Cross Sections for H$_2$ and D$_2$

E. Krishnakumar,[1,2,*] S. Denifl,[3,†] I. Čadež,[4,‡] S. Markelj,[4,§] and N. J. Mason[2,||]

[1]*Tata Institute of Fundamental Research, Mumbai, India 400005*
[2]*Department of Physics and Astronomy, The Open University, Walton Hall, Milton Keynes, MK7 6AA, United Kingdom*
[3]*Institute of Ion Physics and Applied Physics, University of Innsbruck, Technikerstrasse 25, A-6020 Innsbruck, Austria*
[4]*Jožef Stefan Institute, Jamova cesta 39, 1000 Ljubljana, Slovenia*

New measurements of the absolute cross sections for dissociative electron attachment (DEA) in molecular hydrogen and deuterium are presented which resolve previous ambiguities and provide a test bed for theory. The experimental methodology is based upon a momentum imaging time-of-flight spectrometer that allowed us to eliminate any contributions due to electronically excited metastable neutrals and ultraviolet light while ensuring detection of all the ions. The isotope effect in the DEA process in the two molecules is found to be considerably larger than previously observed. More importantly, it is found to manifest in the polar dissociation process (also known as ion pair production) as well.

PACS numbers: 34.80.Ht

Dissociative electron attachment (DEA) in hydrogen is of fundamental importance as one of the benchmark cases in atomic collisions. Together with its reverse process of associative detachment (AD), it is also relevant to the studies in astrophysics [1–3], development of ion sources [4], and in fusion edge plasmas [5,6]. Three distinct resonant processes leading to negative ion production (H$^-$ and/ or D$^-$) were studied and absolute cross sections (CSs) for DEA in H$_2$, $e + H_2 \rightarrow H_2^- \rightarrow H + H^-$, and its isotopologues HD and D$_2$ have been reported. These three processes are believed to proceed through the lowest attractive $X^2\Sigma_u^+$ state (4 eV process), the repulsive $B^2\Sigma_g^+$ state (7–13 eV process), and the attractive Rydberg excited state, $2\Sigma_g^+$ (14 eV process) leading to excited H (D). The peak cross section for the most abundant process at 14 eV in H$_2$ DEA was determined in two independent measurements to be 3.5×10^{-20} cm^2 [7] and 2.1×10^{-20} cm^2 [8]. These two CS values were the only ones available until now and therefore have been widely quoted and used in many applications. More recently, the CS for the 14 eV process was used to normalize the CS for the 4 eV process in relative CS studies [9,10]. It should be noted that the unusually small number of DEA CS measurements in hydrogen and the still high uncertainty in the CS is mainly due to its very low value. For example, the peak CS for H$_2$ DEA is 2 orders of magnitude smaller as compared to O$_2$ DEA. Another important characteristic of DEA in hydrogen is a strong decrease in the CS for heavier isotopologues, HD and D$_2$ [8,9], due to the strongly reduced survival probability of the dissociative channel.

Additional data on DEA in hydrogen have been provided by other experiments: H$^-$ angular distributions [11], the strong dependence of DEA at 4 eV on rovibrational excitation [12], and the appearance of interference structures in the CS between 8–12 eV [11] and at 14 eV [13].

Two more studies on the relative DEA cross section have been performed with emphasis on the vibrational excitation dependency of the 14 eV resonance in H$_2$ and D$_2$ [14] and on the electron energy resolution dependency of the experimental CS for the 4 eV process in H$_2$ [10]. Because of the increase of the DEA CS by orders of magnitude with vibrational excitation of the target molecule [12,15], DEA in hydrogen has to be taken into account in the modeling of low temperature plasmas. This is also well recognized in modeling the edge plasma in tokamak fusion reactors, e.g., [16], where, besides the strong increase of CS with excitation, the pronounced isotope effect will also influence the plasma behavior. Besides its importance in the various research fields of physics mentioned before, the availability of accurate DEA cross section is also crucial for numerous theoretical studies of DEA in hydrogen, e.g., [15,17,18].

In addition to the large discrepancy between two existing experimental absolute values for 14 eV, the previous data also revealed a strong monotonic increase in the ion signal for incident electron energies above 11 eV which is superimposed upon the resonant ion signal from DEA. Previously [8] it was suggested that the underlying background signal may arise from scattered electrons and electrons emitted by ionization of H$_2$. However, another process demonstrating a monotonically increasing CS which may contribute to the signal is polar dissociation, $e + H_2 \rightarrow e + H^+ + H^-$. This process can be excluded below about 17.2 eV, which is the threshold for polar dissociation in hydrogen. As discussed in [19], the background may arise from UV light by deexcitation of electronically excited hydrogen or by metastable molecules. In the present study we determined the absolute CS for DEA to H$_2$ and D$_2$ utilizing an experimental setup where background contributions from UV photons and excited

neutrals are avoided and collection of all ions is ensured. The latter is a crucial point for DEA in hydrogen; for example, the broad resonance peaking at 10 eV produces H^-/D^- ions with kinetic energy of as much as 4 eV. We observe that the absolute CSs for both H_2 and D_2 are significantly lower than in previous investigations. The data also reveal an isotope effect in polar dissociation.

In the present experiment, carried out at the Open University, we used a momentum imaging time-of-flight (TOF) spectrometer. Briefly, 100 ns wide pulses of a magnetically collimated and pulsed electron beam interact with an effusive molecular beam at room temperature produced by a capillary tube. The ions formed in the collision region are extracted into a velocity map imaging (VMI) TOF spectrometer using a pulsed electric field within 10–20 ns after the electron pulse. The VMI spectrometer is similar to the one reported earlier [20], but with a longer flight tube (20 cm) for better mass separation and a larger detector of 75 mm diameter made of three microchannel plates in a Z-stack configuration and a phosphor screen. The experiment was performed in an oil-free vacuum system with a base vacuum of a few times 10^{-9} Torr. The magnetic field (30 G) used for collimating the electron beam is produced by a pair of Helmholtz coils mounted outside the vacuum chamber. The biases on the detector and the phosphor screen can be pulsed simultaneously with a 2 kV pulse to detect ions of given mass to charge ratio or even selectively detect the central slice of the Newton sphere of that particular ion species by controlling the width of the pulse. The images on the phosphor screen are recorded using a CCD camera. The spectrometer can also be used as a simple TOF spectrometer in ion counting mode with the detector continuously biased. The extraction field and the VMI spectrometer biases are optimized for imaging even the high kinetic energy H^- ions produced across the broad resonance, thus ensuring that all the ions are extracted and transported to the detector. The entire set of measurements was carried out under these conditions. The TOF technique allows the separation of any contributions from UV photons and metastable particles to the ion signal. UV photons from the allowed transitions are emitted promptly on a nanosecond time scale. On the other hand, metastable molecules and atoms are slow compared to the accelerated ions and thus will eventually contribute only a negligible amount to the overall background.

For CS measurements, the pulses from the detector are used to generate the TOF spectrum using a time to amplitude converter. The ion yield curves are obtained by selecting the appropriate mass from the TOF spectrum. These curves are normalized to absolute values using the relative flow technique [21] with O^- from O_2 as the standard [22]. Any discrimination in the detection efficiency between H^- and O^- ions was eliminated by monitoring their intensities as a function of the detector bias and ensuring saturation of the detector efficiency at the bias voltage used for the final

measurements. The errors in the measurements are due to statistical errors from the ion counting, errors in the pressure measurement used in the relative flow technique, errors in the electron current measurement, and the uncertainty in the O^- CS from O_2. The upper limit of uncertainty (1σ) in our measurements is therefore estimated to be 12%, with the dominant contribution arising from the 10% uncertainty in the O^- data [22].

The above O_2 data were obtained by Rapp and Briglia [22] using the same technique with which they measured the H_2 DEA cross sections. The systematic error due to UV and metastable atoms and molecules in O_2 data would be much smaller than the stated uncertainty of 10% in their data. This is due to the 2 orders of magnitude bigger CS in O_2 than in H_2 and to the lower DEA threshold energy in O_2. The cross section in O_2 has a pure bell shape with no apparent background at the higher energy side. There are six other reports on the O_2 DEA cross sections and, barring one, they all agree with the results of Rapp and Briglia within 10% [23].

The momentum image of H^- ions at an incident electron energy of 11 eV is shown in Fig. 1. It shows that all the H^- ions formed in the interaction region are transported to the detector, irrespective of their initial momenta. At 11 eV electron energy the kinetic energy of the H^- ions is slightly larger than 3.5 eV. It can be seen from the image that even ions of considerably larger kinetic energy could be detected under the conditions we employed for our measurements. Thus the momentum imaging has provided conclusive evidence that we are not discriminating ions based on their kinetic energies.

The cross sections for H^- from H_2 are shown in Fig. 2 together with previous results. Among the previous measurements, only those by Schulz [7] and Rapp et al. [8] are absolute measurements. Both Schulz and Asundi [9] and Drexel et al. [10] used the data of Rapp et al. at 14 eV (which is 2.1×10^{-20} cm^2) to normalize their data at 4 eV. We obtain a peak cross section of 1.6×10^{-21} cm^2 for the
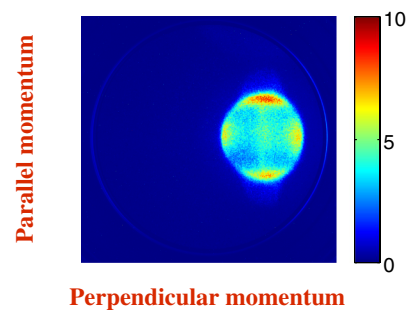

FIG. 1 (color online).　Momentum image of H^- from H_2 at 11 eV electron energy. This image proves that all the H^- ions are transported to the detector. The narrow outer ring is due to the reflection at the glass boundary of the phosphor screen. The image is shifted to the right due to the effect of the magnetic field on the ions.
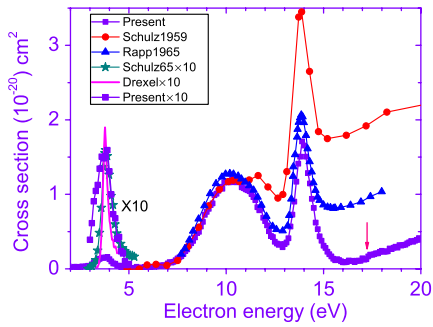
FIG. 2 (color online).   Absolute cross section for the formation of H^- from H_2. Circles—from Ref. [7], triangles—from Ref. [8], stars—from Ref. [9], solid line—from Ref. [10], and squares—present results. The arrow indicates the polar dissociation threshold. Also shown are the data in the 3–5 eV range after multiplication by a factor of 10, as indicated in the figure, for clarity.

4 eV resonance. Our results are compared with the theoretical CS of Horacek *et al.* [15] in Fig. 3 after convoluting their CS by a Gaussian energy distribution of full width at half maximum (FWHM) = 0.753 eV. It had to be multiplied by a factor of 0.7 in order to reproduce the present experiment. The experimental energy distribution was determined by the analysis of the vertical onset of the O^- current produced from DEA in CO under identical experimental conditions. We also note that convolution of theoretical CS by a thermionic distribution of 0.840 eV could reproduce experimental data points better, and such a fit multiplied by 0.8 is also shown in Fig. 3. Thus the present experimental CS is lower than that of Horacek *et al.* by 20%–30%. Our results are in better agreement with more recent calculations employing an alternative method which also included contribution from the direct
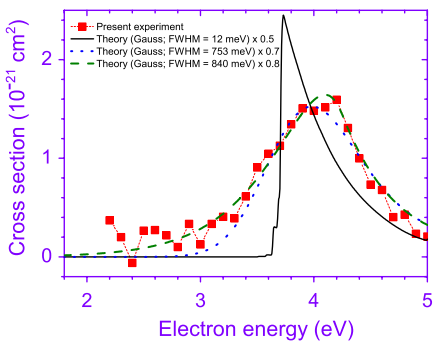

FIG. 3 (color online).   Comparison of the present cross section for the 4 eV resonance with the theoretical results. Solid line—theoretical data [15] convoluted with a Gaussian electron energy spread of 12 meV and multiplied by a factor 0.5, dotted line—theoretical data [15] convoluted with a Gaussian of FWHM of 0.753 eV and multiplied by a factor of 0.7, dashed line—theoretical data [15] convoluted with a thermionic electron energy spread of 0.840 eV and multiplied by a factor of 0.8, and squares—present results.

scattering [17]. Recent measurements of the rate coefficient for AD in hydrogen, $H^- + H \rightarrow H_2 + e^-$ [2,24], agreed very well with theoretical ones based on the same model as the one used in [15]. It is important to note that although both processes, DEA and AD, proceed through the same resonant state, they take place in different regions of internuclear separation.

For the broad resonance between 7 and 13 eV we observe good agreement between our results and that of Schulz [7] up to 11 eV. Beyond 11 eV, the data of Schulz appear to diverge drastically from the present data. At this resonance the data of Rapp *et al.* [8], though higher, are in agreement with ours up to 12 eV within the combined experimental errors. Beyond 12 eV, their data also appear to diverge from ours, though not as rapidly as that of Schulz. This is manifested in the differences in the cross section at 14 eV, where the CS of Rapp *et al.* is 24% higher than what we observe, while that of Schulz is larger by a factor of 2. In comparison to the present results, the cross sections from these two measurements continue to diverge as the energy is increased beyond 14 eV. While we are able to see clearly the threshold for the polar dissociation continuum, both these measurements do not show such a threshold, strongly suggesting considerable contamination due to UV and metastable molecules. This contamination may also explain the observed deviation beyond 11 eV as both the UV and metastable molecule production start around this energy [19,25]. Recent CS calculations of the 14 eV DEA using a simple local complex potential model [18] and convolved with an energy spread of 300 meV were in agreement with the first measurements of Schulz [7] but are in disagreement with our results. This may be due to the fact that the calculations neglected the predissociation decay channel of the resonant state above 14 eV, which is evident in the high resolution H^- yield [13].

The results for D_2 are presented in Fig. 4 along with those from Rapp *et al.* [8]. The cross sections from H_2 divided by a factor of 3 are also given for comparison. We are unable to see any D^- signal above the noise level at the
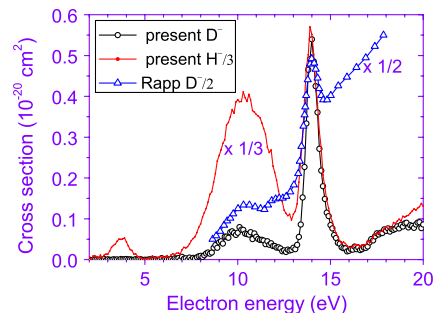

FIG. 4 (color online).   Absolute cross section for the formation of D^- from D_2. Triangles—from Ref. [8] divided by a factor of 2, and circles—present results. Also given is the cross section for H^- from H_2 (solid line) divided by a factor of 3 for comparison.

4 eV resonance. The CSs from [8] are about a factor of 2 larger at 14 eV and are much larger at other energies. This difference is considerably larger than in the case of H_2. This may be explained in terms of contamination from hot neutrals and UV very similar to that in H_2, but in relative terms much larger than the smaller DEA cross section for D_2. As seen from the figure, the difference in the cross sections for H_2 and D_2 due to the isotope effect is a factor of 3 at the 14 eV resonance, and about a factor of 18 at the 10 eV resonance. These differences are considerably larger than those reported earlier [8].

We also note the presence of the isotope effect in the polar dissociation continuum. So far there has been no report on the isotope effect in the polar dissociation for any molecules by electron impact. There is not much information available about the states that undergo polar dissociation. Guberman [26] has calculated 24 doubly excited states of H_2 which lie above 23 eV and undergo autoionization. The states that undergo polar dissociation, though repulsive in the Franck-Condon region, will have minima at large internuclear separations, due to the $1/r$ potential between the fragments. These states have been shown to behave like a heavy Bohr atom with H^- ion being orbited by a proton with large principal quantum numbers [27,28]. Several states that undergo vibrational autoionization and polar dissociation by photoabsorption in the range of 17.37–17.62 eV have been identified in H_2, HD, and D_2 [29]. Since the polar dissociation process is in competition with the autoionization process, it is similar to the DEA process, except for the difference in the total number of electrons. As in the case of the DEA process, one could define a "survival probability," $p = \exp(-\tau_d/\tau_a)$, such that the state would undergo polar dissociation and not autoionization, where τ_a is the autoionization lifetime and τ_d is the dissociation time. As compared to H_2, τ_d will be larger for D_2 due to larger mass, and hence the survival probability in D_2 will be smaller. Thus the polar dissociation process will have an isotope effect as observed in the present experiment. A subtle difference from the DEA process is that even after surviving autoionization the state may still decay through dissociation into two neutral species instead of polar dissociation. However, this may not affect the isotope dependence in the polar dissociation cross section. Photoionization measurements [29] reported the polar dissociation cross section for H_2 to be larger by a factor of 3–4 as compared to that for D_2, which appears to be in good agreement with the present results. We believe that the difference in the relative shapes of the polar dissociation continuum beyond 18 eV is due to varying contribution from different states that undergo polar dissociation.

*ekkumar@tifr.res.in
†stephan.denifl@uibk.ac.at
‡iztok.cadez@ijs.si
§sabina.markelj@ijs.si
‖n.j.mason@open.ac.uk

[1] S. C. Glover, D. W. Savin, and A.-K. Jappsen, Astrophys. J. **640**, 553 (2006).
[2] H. Kreckel et al., Science **329**, 69 (2010).
[3] D. Field, Astron. Astrophys. **362**, 774 (2000).
[4] M. Bacal, Nucl. Fusion **46**, S250 (2006).
[5] U. Fantz et al., J. Nucl. Mater. **290–293**, 367 (2001).
[6] F. Taccogna et al., Contrib. Plasma Phys. **48**, 147 (2008).
[7] G. J. Schulz, Phys. Rev. **113**, 816 (1959).
[8] D. Rapp, T. E. Sharp, and D. D. Briglia, Phys. Rev. Lett. **14**, 533 (1965).
[9] G. J. Schulz and R. K. Asundi, Phys. Rev. **158**, 25 (1967).
[10] H. Drexel et al., J. Phys. B **34**, 1415 (2001).
[11] M. Tronc, F. Fiquet-Fayard, C. Schermann, and R. I. Hall, J. Phys. B **10**, 305 (1977).
[12] M. Allan and S. F. Wong, Phys. Rev. Lett. **41**, 1791 (1978).
[13] M. Tronc, R. I. Hall, C. Schermann, and H. S. Taylor, J. Phys. B **12**, L279 (1979).
[14] I. Čadež, R. I. Hall, M. Landau, F. Pichou, and C. Schermann, J. Phys. B **21**, 3271 (1988).
[15] J. Horáček, M. Čížek, K. Houfek, P. Kolorenč, and W. Domcke, Phys. Rev. A **70**, 052712 (2004).
[16] D. Reiter et al., J. Nucl. Mater. **363–365**, 649 (2007).
[17] D. Rabli and M. A. Morrison, Phys. Rev. Lett. **97**, 013201 (2006).
[18] R. Celiberto, R. K. Janev, J. M. Wadehra, and A. Laricchiuta, Phys. Rev. A **80**, 012712 (2009).
[19] I. Čadež, S. Markelj, Z. Rupnik, and P. Pelicon, J. Phys. Conf. Ser. **133**, 012029 (2008).
[20] D. Nandi, V. S. Prabhudesai, A. Chatterjee, and E. Krishnakumar, Rev. Sci. Instrum. **76**, 053107 (2005).
[21] E. Krishnakumar and K. Nagesha, Rapid Commun. Mass Spectrom. **9**, 336 (1995).
[22] D. Rapp and D. D. Briglia, J. Chem. Phys. **43**, 1480 (1965).
[23] L. G. Christophorou, R. N. Compton, G. S. Hurst, and P. W. Reinhardt, J. Chem. Phys. **43**, 4273 (1965).
[24] H. Bruhns et al., Phys. Rev. A **82**, 042708 (2010).
[25] Jung-Sik Yoon et al., Rep. Prog. Phys. **73**, 116401 (2010).
[26] S. L. Guberman, J. Chem. Phys. **78**, 1404 (1983).
[27] M. O. Vieitez, T. I. Ivanov, E. Reinhold, C. A. de Lange, and W. Ubachs, Phys. Rev. Lett. **101**, 163001 (2008).
[28] A. Kirrander, J. Chem. Phys. **133**, 121103 (2010).
[29] W. A. Chupka, P. M. Dehmer, and W. T. Jivery, J. Chem. Phys. **63**, 3929 (1975).